Power Loss Minimization of Off-Grid Solar DC Nano-Grids—Part I: Centralized Control Algorithm

Cephas Samende, *Student Member, IEEE,* Sivapriya M. Bhagavathy, *Member, IEEE,* and Malcolm McCulloch, *Senior Member, IEEE*

***Abstract*—Peer-to-peer interconnection of households having on-site batteries, multi-port converters and solar panels to form a multi-port converter-enabled solar DC nano-grid is an emerging approach for providing affordable energy access in rural areas. Battery charge and discharge losses, distribution losses and converter losses are significant problem when operating such nano-grids. This paper presents a centralized control algorithm that can help address the power loss problem. The proposed algorithm uses a new problem formulation where the power loss problem is formulated as a two-stage convex optimization problem. The first stage of the optimization problem is an optimal battery dispatch problem for determining optimal battery charge and discharge currents. The second stage is an optimal current flow problem for determining optimal distribution voltages which corresponds to the optimal battery currents. Simulation results of the nano-grid show that the proposed algorithm can minimize the nano-grid power losses while facilitating the power exchange between the households. The proposed algorithm is suitable for small nano-grids where privacy of households is not a concern. In Part II of this paper we propose a distributed control algorithm that preserves the privacy of the households especially where the size of the nano-grid is large.**

***Index Terms*—Multi-port converter, solar DC nano-grid, energy access, power loss, centralized control algorithm.**

NOMENCLATURE

$R_{dc,i}$	Distribution line resistance
$r_{b,i}$	Battery's internal resistance at time t
$v_{dc,i}$	Distribution voltage at time t
$V_{dc,i}$	Constant distribution voltage
$V_{dc,n}$	Nominal distribution voltage
$v_{b,i}$	Battery terminal voltage at time t
$v_{pv,i}$	Solar panel terminal voltage at time t
$v_{L,i}$	Load terminal voltage at time t
$v^{b}_{oc,i}$	Battery's open circuit voltage at time t
$v^{dc}_{min,i}$	Minimum distribution voltage
$v^{dc}_{max,i}$	Maximum distribution voltage
$V^{b}_{n,i}$	Nominal battery voltage
$C_{b,i}$	Battery capacity
$i_{dc,i}$	Distribution line current at tme t
$i_{b,i}$	Battery charge/discharge current at time t
$I_{b,i}$	Referred battery charge/discharge current
$P_{b,i}$	Battery power output at time t
$P_{L,i}$	Load power at time t
$P_{pv,i}$	Solar power at time t
$P^{c}_{loss,i}$	Converter loss at time t

The authors are with the Department of Engineering Science, Energy and Power Group, University of Oxford, Oxford, UK e-mail: {cephas.samende, sivapriya.mothilalbhagavathy, malcolm.mcculloch} @eng.ox.ac.uk.

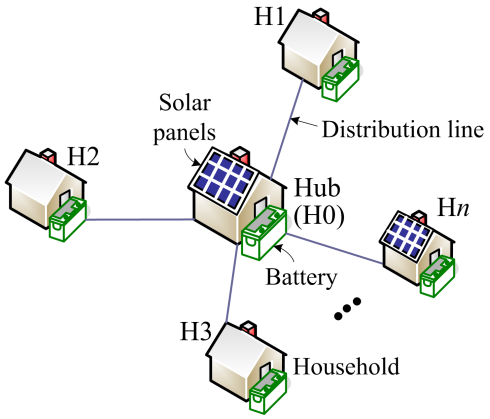

Fig. 1. Diagram of a multi-port converter-enabled off-grid solar DC nano-grid.

$P^{-}_{c,i}$	Converter's minimum power output
$P^{+}_{c,i}$	Converter's maximum power output
Δt	Battery charge/discharge time step
e_{λ}	Convergence factor
$SoC_{0,i}$	Battery's initial State of Charge (SoC)
SoC_{i}	Battery's SoC at time t
$SoC_{min,i}$	Battery's minimum SoC
$SoC_{max,i}$	Battery's maximum SoC
λ	Lagrange multiplier for equality constraint
μ_i, σ_i	Lagrange multipliers for inequality constraints
$\eta^{ch}_{b,i}, \eta^{dis}_{b,i}$	Battery charge and discharge efficiency
$\alpha_i, \beta_i, \gamma_i$	Power loss coefficients

I. INTRODUCTION

THIS paper aims to develop a centralized control algorithm that can minimize power losses of solar DC nano-grids that are designed for energy access.

Concerns of climate change and scattered populations have made the electrification of rural areas through grid extension difficult and expensive [1]. One innovative and affordable solution for providing energy access to rural areas is through swarm electrification approach [2]. The approach seeks to electrify rural areas by gradually interconnecting households that have stand-alone systems such as solar home systems [3] and rechargeable batteries to form a diverse peer-to-peer grid (hereafter referred to as a solar DC nano-grid) as shown in Fig. 1. In this paper, every household and hub uses a multi-port converter (e.g. Four-Port DC-DC Converter (FPC) [4]) to manage power flow. This is referred to as a multi-port converter-enabled solar DC nanogrid, shown in Fig. 1. The

Samende, C., Bhagavathy, S. M., & McCulloch, M. (2021). Power loss minimization of off-grid solar DC nano-grids—part I: centralized control algorithm. IEEE Transactions on Smart Grid, 12(6), 4715-4725. https://doi.org/10.1109/TSG.2021.3108236

use of multi-port converters offer advantages such as galvanic isolation and reduced cabling costs compared to single input, single output converters [5].

Electrification of rural areas through multi-port converter-enabled solar DC nano-grids supports the bidirectional exchange of energy between households and offers advantages in terms of productive uses of energy, opportunity for energy trading and increased diversity in power generation and consumption [6]. However, it also introduces operational challenges in terms of power losses which include distribution line losses [7], battery charge and discharge losses [8] and converter losses [4], which occur during the process of power distribution. Power losses reduce the energy efficiency of nano-grids. Studies indicate that a 1.2% improvement in the global energy efficiency is equivalent to a gain in global GDP of about US$1.6 trillion [9]. Owing to lack of national grid connection and the limited generation capacity of nano-grids, there is need to minimize the power losses through an appropriate control algorithm to save energy and make the nano-grids more affordable for energy access.

Developing a control algorithm to address the power loss problem is a non-trivial task for several reasons. Firstly, lack of national grid connection and intermittency of solar power requires a highly accurate control algorithm in order to avoid power supply-demand imbalance in the nano-grid. Secondly, the need to keep the battery charge and discharge power and State of Charge (SoC) within a certain range to enhance the lifetime of the battery [10] increases the computational time of the control problem. Lastly, DC power flow on a distribution line is non-linear and non-convex, making the power loss problem a computational challenge [11].

Given that the concept of solar DC nano-grids is relatively new, having officially come to light in 2012 [12], most of the research focus has been on the feasibility of the concept [13], design and sizing [3], modelling under droop control [14], technical benefits [6], and financial benefits [15]. Few studies have attempted to consider the nano-grid power loss problem. In [16], a data analysis tool which optimizes the distribution network topology of the nano-grid is developed with the aim of achieving an efficient power flow between the households. A distribution loss analysis is presented in [17] for optimally planning and designing a DC micro-grid (DCMG) architecture with minimum distribution losses.

While the aforementioned research focused on optimal planning and designing of the nano-grids, it is to the best knowledge of the author that there are no studies that focus on developing control algorithms that address the power loss problem of operational solar nano-grids. The few existing control methods in literature focus on addressing the power loss problem of interconnected DC clusters [18], conventional DCMGs [19] and High Voltage Direct Current (HVDC) systems [20] as follows.

In [18] a decentralized voltage control method is proposed to efficiently coordinate the power exchange between two autonomous DC clusters. Transmission loss between the two DC clusters is shown to be reduced. However, how to minimize the distribution losses, battery losses and converter losses within each DC cluster is not considered. In [21], a decentralized voltage control method which works in a perturb and observe manner is proposed to minimize distribution losses in an islanded DCMG. Battery and converter losses are however not considered. An optimal power flow based control scheme is proposed in [20] to minimize power losses in multi-terminal HVDC systems for offshore wind power plants. Transmission losses are considered in the control scheme while battery and converter losses are ignored. A dynamic optimal power flow strategy with the objective of minimising the battery losses and distribution line losses of a DCMG is proposed in [8]. The strategy first converts the non-convex power loss problem to a convex problem through linearisation of power flow equations and then solved using commercial solvers. However, converter losses are ignored and the linearisation of the power flow equations can lead to less accurate results and high computational times. Other control algorithms include greedy algorithms in [22] and heuristic methods such as genetic algorithms in [23]. However, greedy algorithms are reported in [22] to be sub-optimal when there are few participating households. In addition, greedy algorithms can lead to overuse of batteries in households which are close together, requiring frequent battery replacements, which can be expensive. Heuristic methods e.g. in [23] on the other hand tend to be slow since they involve exploring the search space in many directions.

In this paper, an iterative solving algorithm is proposed to minimize the nano-grid power losses while satisfying operational constraints such as the battery SoC. The contributions of this paper are as follows:

- A simplified FPC power loss model which is capable of providing real time FPC power loss estimations is developed from experimental results.
- A novel and comprehensive mathematical formulation of the nano-grid power loss problem is developed, taking all the three types of nano-grid power losses into account.
- The nano-grid power loss problem is decomposed into two interdependent sub-problems; the Optimal Battery Dispatch Problem (OBDP) and Optimal Current Flow Problem (OCFP). Thus, complex linearisation [8] and relaxation of power flow equations are not required.
- A centralized control algorithm which consists of a Fast Lambda Iteration Algorithm (FLIA) and a Fast Voltage Iteration Algorithm (FVIA) is developed to address the nano-grid power loss problem.

The rest of the paper is organised as follows. Section II presents a model of the nano-grid. Section III describes the formulation of the power loss optimization problem. Section IV presents the proposed control algorithm. Simulation results that verify the performance of the proposed method are given in Section V. Section VI concludes the paper.

II. System Model

Fig. 1 shows the multi-port converter-enabled solar DC nano-grid considered in this paper. It consists of multiple households (labelled H1 to Hn) that are connected to a central hub (H0) in a spoke and hub manner in order to lower the cost associated with the distribution lines. To lower the upfront investment costs, only the hub has both mandatory

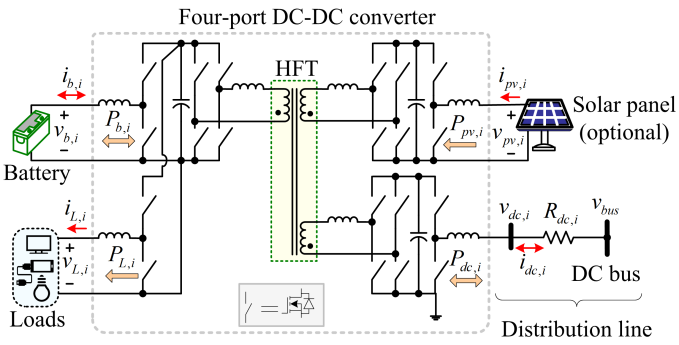

Fig. 2. Integration of the (optional) solar panel, battery, DC loads and distribution line in every household/hub, H*i* of the nano-grid using a FPC.

solar panels and batteries while solar panels remain optional at the households. FPCs are used as multi-port converters to manage the power flow in the nano-grid by integrating its key components i.e. batteries, (optional) solar panels, DC loads and distribution lines in every household and hub, H*i*, as shown in Fig. 2.

Each terminal (port) of the FPC is controlled independently without affecting operation of devices connected to other terminals. The load port is controlled to maintain a constant load voltage (e.g. 12 V), since most DC loads in rural areas such as light emitting diode bulbs can operate at constant voltage. The solar port can be independently controlled to either maintain a net zero power injection (in the case of households without solar panels) or operate in maximum power point tracking mode by tracking the appropriate solar panel voltage (if a household/hub has solar panels). The battery port is not directly regulated and serves as a slack terminal, absorbing and supplying any power imbalance in the network. Power exchange between the hub and households is achieved by regulating the distribution line voltage. This implies that to minimize the power losses in the nano-grid, optimal distribution line voltages should be determined. To formulate and subsequently solve the nano-grid power loss problem, the nano-grid must be modelled first as follows.

A. Distribution Line Model

Every distribution line connecting a household to the hub is modelled by its resistance, $R_{dc,i}$. In the hub, these distribution lines are connected to a common DC bus bar having voltage, v_{bus} as shown in Fig. 2. The current, $i_{dc,i}$ received by H*i* from the distribution line is calculated as

$$i_{dc,i} = \left(v_{bus} - v_{dc,i}\right)/R_{dc,i} \quad i = 1, 2, \ldots, n \tag{1}$$

Applying Kirchhoff's Current Law (KCL) at the DC bus and taking $R_{dc,0}$ to be zero, $i_{dc,0} = -\sum_{i=1}^{n} i_{dc,i}$ and v_{bus} is obtained as

$$v_{bus} = v_{dc,0} = \left(\sum_{i=1}^{n} \frac{v_{dc,i}}{R_{dc,i}} - i_{dc,0}\right) \Big/ \sum_{i=1}^{n} \frac{1}{R_{dc,i}} \tag{2}$$

B. Solar Panel Model

Solar panels directly convert solar irradiance and temperature into DC power, $P_{pv,i}$ and voltage, $v_{pv,i}$. The solar panel model presented in [24] is used in this paper.

C. Load Model

Constant-power loads that include motoring loads such as sewing machines and water pumps, lighting loads such as light emitting diode lights and electronic loads such as Television sets, radios and cell phone chargers are the common DC loads in rural areas that require energy access [25]. Other load types which include constant-current loads such as welding machines and constant-impedance loads such as stove tops and water heaters are not a priority in rural areas needing energy access and hence not common. For this reason, the FPC considered in this paper was designed for constant-power loads only where the load voltage $v_{L,i}$ is regulated to maintain a constant value. However, it should be noted that the formulations that are presented in this paper are carried out at steady-state and applicable to any load type since only the load power, $P_{L,i}$ is of interest. Performance of the proposed method for various load types at low-level time scales is beyond the scope of this paper.

D. Battery Model

Key properties of a battery are its cell open circuit voltage, $v^b_{oc,i}$, cell internal resistance, $r_{b,i}$ and SoC, SoC_i. The $v^b_{oc,i}$ and $r_{b,i}$ are related to SoC_i as given in (3) [8].

$$\begin{cases} v^b_{oc,i} = a_0 e^{-a_1 SoC_i} + a_2 + a_3 SoC_i - a_4 SoC_i^2 + a_5 SoC_i^3 \\ r_s = b_0 e^{-b_1 SoC_i} + b_2 + b_3 SoC_i - b_4 SoC_i^2 + b_5 SoC_i^3 \\ r_{ts} = c_0 e^{-c_1 SoC_i} + c_2\,, \quad r_{tl} = d_0 e^{-d_1 SoC_i} + d_2 \\ r_{b,i} = r_s + r_{ts} + r_{tl} \end{cases} \tag{3}$$

where $a_0, \ldots, a_5$, $b_0, \ldots, b_5$, $c_0, \ldots, c_2$ and $d_0, \ldots, d_2$ are coefficients (of 860 mAh, 3.7 V Lithium-ion battery cell), which are given in Table I. The battery cell current, $i_{cell,i}$

TABLE I
BATTERY COEFFICIENTS [8]

a_0	-0.852	a_1	63.867	a_2	3.6297	a_3	0.559
a_4	0.510	a_5	0.508	b_0	0.1463	b_1	30.27
b_2	0.1037	b_3	0.0584	b_4	0.1747	b_5	0.1288
c_0	0.1063	c_1	62.94	c_2	0.0437	d_0	-200
d_1	-138	d_2	300				

for a given $P_{b,i}$ can be obtained as

$$i_{cell,i} = 0.5 v^b_{oc,i}/r_{b,i} - 0.5\sqrt{\left(v^b_{oc,i}/r_{b,i}\right)^2 - 4P_{b,i}/\left(N_s N_p r_{b,i}\right)} \tag{4}$$

where $N_s = V^b_{n,i}/3.7$ and $N_p = C_{b,i}/0.86$ are numbers of equivalent 860 mAh, 3.7 V Lithium-ion battery cells connected in series and parallel respectively. The SoC_i is estimated in discrete time domain [26] as

$$SoC_i = \begin{cases} SoC_{0,i} - \eta^{ch}_{b,i} P_{b,i} \Delta t / C_{b,i}\,, & P_{b,i} < 0 \\ SoC_{0,i} - P_{b,i} \Delta t / \left(\eta^{dis}_{b,i} C_{b,i}\right)\,, & P_{b,i} \geq 0 \end{cases} \tag{5}$$

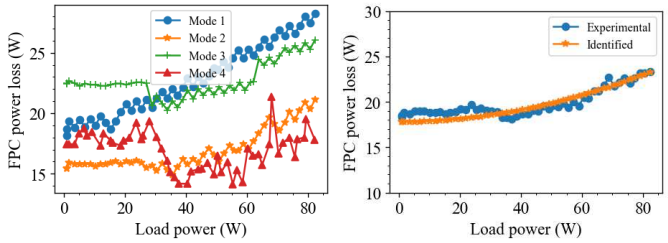

(a) (b)

Fig. 3. Variation of FPC loss with load power: (a) experimental FPC loss curves for four operating modes and (b) average experimental FPC loss and identified FPC loss curves.

The $\eta_{b,i}^{ch}$ and $\eta_{b,i}^{dis}$ can be calculated as

$$\eta_{b,i}^{ch} = v_{oc,i}^{b}/v_{b,i}\,, \quad \eta_{b,i}^{dis} = v_{b,i}/v_{oc,i}^{b} \tag{6}$$

where $v_{b,i}$ for a given $P_{b,i}$ can be calculated as

$$v_{b,i} = P_{b,i}/i_{b,i}\,, \quad (i_{b,i} = N_p i_{cell,i}) \tag{7}$$

E. Four-port DC-DC Converter Model

The structure of the considered FPC is shown in Fig. 2. The key physical phenomenon of the FPC is the power loss which occurs as currents and voltages are converted from one form to another. To obtain the FPC loss, four main operating modes of the FPC were considered:

1) *Mode 1:* Battery supplying the DC load while power from the solar panel and distribution line was zero.
2) *Mode 2:* Battery and distribution line supplying the DC load while power from the solar panel was zero.
3) *Mode 3:* Battery and solar panel supplying the DC load while power from the distribution line was zero.
4) *Mode 4:* Battery, solar panel and distribution line all supplying the DC load.

The aforementioned modes are the extreme operating modes of the FPC. The other operating modes of the FPC are a combination of the above modes and their resulting FPC loss were considered to be between those of the aforementioned operating modes. Increasing the load power from 1 W to 82 W for each of the modes, the FPC loss was obtained as shown in Fig. 3a. As shown in Fig. 3a, FPC loss for each of the modes varied as a quadratic function of the load power. Thus, without loss of generation, it was possible to obtain an average experimental FPC loss as shown in Fig. 3b, which is an approximation of the FPC loss for all the FPC operating modes. Using curve fitting techniques as shown in Fig. 3b, the identified FPC loss was expressed as a quadratic function of load power, $P_{L,i}$ as follows

$$p_{loss,i}^{c} = 17.765 + 0.00175P_{L,i} + 0.000791P_{L,i}^{2} \tag{8}$$

The simplified FPC loss (8) is good enough to be used in the formulation of a convex power loss optimization problem compared to the non-linear approach proposed in [4].

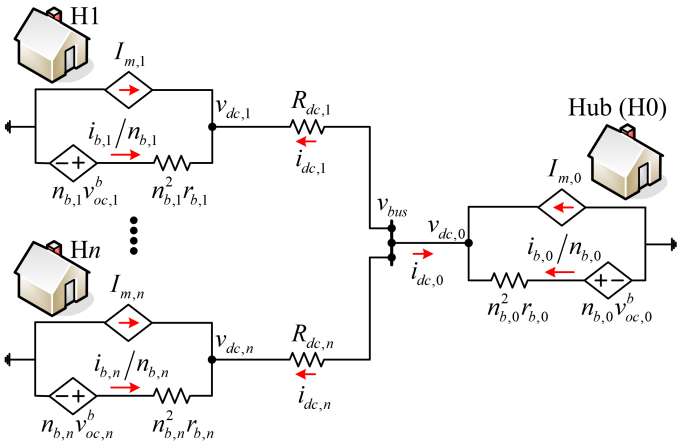

Fig. 4. Equivalent circuit model of a FPC-enabled solar DC nano-grid.

F. Solar DC Nano-Grid Model

Since $P_{pv,i}$ and $P_{L,i}$ are externally determined from atmospheric weather conditions and power consumption respectively, and that $p_{loss,i}^{c}$ is a function of $P_{L,i}$, these are treated as constants at every time instant. Denoting the ratio of $v_{dc,i}$ to $v_{b,i}$ as $n_{b,i}$ in Fig.2, the battery's $v_{oc,i}^{b}$ and $r_{b,i}$ at the FPC battery port can be moved to the distribution line side of the FPC to form the nano-grid equivalent circuit model as shown in Fig. 4. Here, the (referred) battery output current and power is given as

$$I_{b,i} = i_{b,i}/n_{b,i} \tag{9a}$$

$$P_{b,i} = I_{b,i}v_{dc,i} \tag{9b}$$

The mismatch current, $I_{m,i}$ is the difference between $P_{pv,i}$, $P_{L,i}$ and $p_{loss,i}^{c}$ as follows

$$I_{m,i} = \left(P_{pv,i} - P_{L,i} - p_{loss,i}^{c}\right)/v_{dc,i} \tag{10}$$

For households without a solar panel, $P_{pv,i} = 0$ in (10). The current, $i_{dc,i}$ received by each Hi, $i = 0, \ldots, n$ in Fig. 4 must satisfy the KCL as follows

$$i_{dc,i} = -I_{m,i} - I_{b,i} \tag{11}$$

By conservation of current, the algebraic sum of currents, ΔI in the nano-grid must be equal to zero as follows

$$\Delta I = \sum_{i=0}^{n} i_{dc,i} = \sum_{i=0}^{n} \left(I_{D,i} - I_{b,i}\right) = 0\,, \quad (I_{D,i} = -I_{m,i}) \tag{12}$$

III. Optimization Problem Formulation

The main objective of this paper is to minimize the total nano-grid power losses, J. The power losses considered are battery charge and discharge losses, distribution line losses and FPC losses. According to Fig. 4, J can be expressed as

$$J = \sum_{i=0}^{n} \left[\left(-I_{m,i} - I_{b,i}\right)^{2} R_{dc,i} + I_{b,i}^{2} n_{b,i}^{2} r_{b,i} + p_{loss,i}^{c}\right] \tag{13}$$

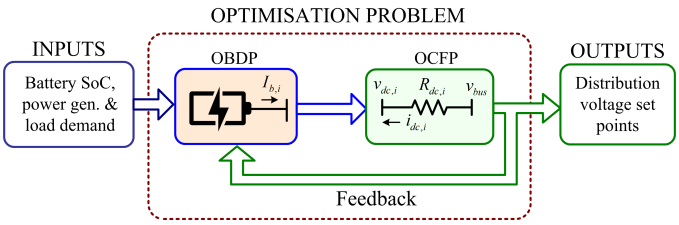

Fig. 5. Decomposition of the solar DC nano-grid power loss optimization problem.

In the considered nano-grid, batteries are the only dispatchable energy sources and power exchange between the households is achieved by regulating the distribution voltages. To minimize the power losses, the batteries must be optimally dispatched and the distribution voltages must be optimally determined. A two-stage power loss optimization problem which consists of two sub-problems, the OBDP and OCFP is proposed. This is presented as a closed loop control system as shown in Fig. 5. The feedback loop helps to keep errors resulting from the proposed formulation to a minimum.

The main objective of the OBDP is to find $\mathbf{I_b} = \left[I^*_{b,0}, \ldots, I^*_{b,n}\right]^T$, a vector of battery charge and discharge currents that minimizes J given by (13) while satisfying some constraints. Using (13) and the expressions developed in Section II, the OBDP is stated as follows

$$\underset{I_b}{\text{minimize:}} \quad J = \sum_{i=0}^{n} \left(\alpha_i I_{b,i}^2 + \beta_i I_{b,i} + \gamma_i\right) \tag{14a}$$

$$\text{subject to:} \quad \sum_{i=0}^{n} I_{b,i} = \sum_{i=0}^{n} I_{D,i} \tag{14b}$$

$$P^b_{min,i} \leq P_{b,i} \leq P^b_{max,i} \tag{14c}$$

$$v^{dc}_{min,i} \leq v_{dc,i} \leq v^{dc}_{max,i} \tag{14d}$$

where

$$\alpha_i = \left(\frac{v_{dc,i}}{v_{b,i}}\right)^2 r_{b,i} + R_{dc,i} \tag{15a}$$

$$\beta_i = \frac{2R_{dc,i}}{v_{dc,i}} \left(P_{pv,i} - P_{L,i} - p^c_{loss,i}\right) \tag{15b}$$

$$\gamma_i = \frac{R_{dc,i}}{v^2_{dc,i}} \left(P_{pv,i} - P_{L,i} - p^c_{loss,i}\right)^2 + p^c_{loss,i} \tag{15c}$$

$$P^b_{max,i} = \min\left(P^+_{c,i}, \frac{\eta^{dis}_{b,i} C_{b,i} \left(SoC_{0,i} - SoC_{min,i}\right)}{\Delta t}\right) \tag{15d}$$

$$P^b_{min,i} = \max\left(P^-_{c,i}, \frac{C_{b,i} \left(SoC_{0,i} - SoC_{max,i}\right)}{\eta^{ch}_{b,i} \Delta t}\right) \tag{15e}$$

Equation (14a) is the objective function of the optimization problem, which in its current form is non-convex due to the non-linear relationship that exists between $v_{dc,i}$, $v_{b,i}$ (which are used to calculate the power loss coefficients; α_i, β_i and γ_i in (15)) and the decision variables, $\mathbf{I_b}$. To convert (14a) to a convex function and (14) to a convex optimization problem thereof, $v_{dc,i}$ and $v_{b,i}$ are treated as constants before each solution iteration and then they get updated for the next solution iteration as discussed in Section IV.

Equation (14b) ensures that currents in the nano-grid are balanced. Inequality (14c) (where $P_{b,i} = I_{b,i} v_{dc,i}$ as given by (9b)) ensures that the battery does not overcharge or over-discharge, which otherwise shortens the lifetime of the battery [10]. It ensures that the minimum SoC, $SoC_{min,i}$, maximum SoC, $SoC_{max,i}$ and converter power limits (i.e. $P^+_{c,i}$ during battery discharging and $P^-_{c,i}$ during battery charging) are satisfied. The second term on the right hand side of equation (15d) places an upper power limit on the battery discharge, and is obtained from (5) for $SoC_i = SoC_{min,i}$. Similarly, a lower power limit is placed on the battery charge through the second term on the right hand side of (15e) for $SoC_i = SoC_{max,i}$.

Lastly, the voltage limits in (14d) ensures that the $v_{dc,i}$ is within the acceptable range where $v^{dc}_{min,i}$ is the lower limit and $v^{dc}_{min,i}$ is the upper limit. In this paper, $v_{dc,i} = V_{dc,i}$ at every iteration to have a convex optimization problem which gets updated at the next iteration.

The main objective of the OCFP is to find distribution voltages, $\mathbf{V_{dc}} = [v_{dc,0}, \ldots, v_{dc,n}]^T$ that corresponds to $\mathbf{I_b}$ obtained from the OBDP (14) by simultaneously solving (1), (2), (10) and (11).

IV. Proposed Control Algorithm

This section presents the proposed centralized control algorithm(see Algorithm 1), which is based on the framework in Fig. 5. It consists of the FLIA and the FVIA which are proposed to solve the OBDP (14) and OCFP at every time instant respectively. In Part II of this paper the OBDP and OCFP will be solved in a distributed manner. Note that (14) can be solved using software packages such as CVXPY [27]. However, software packages usually abstracts (useful) details which are required for deeper understanding of the solution and for designing a distributed control algorithm proposed in Part II of this paper.

A. The Fast Lambda Iteration Algorithm

Since (14) is convex, Karush-Kuhn-Tucker (KKT) optimality conditions are necessary and sufficient conditions for optimality [28]. Without first considering the inequality constraint given by (14c) for convenience, the problem (14) can be converted to an unconstrained optimization problem using the Lagrangian operator L as follows

$$L\left(I_{b,i}, \lambda\right) = J + \lambda \left(\sum_{i=0}^{n} I_{D,i} - \sum_{i=0}^{n} I_{b,i}\right) \tag{16}$$

According to KKT optimality conditions, the operator L is minimized if its partial derivative with respect to each variable, $I_{b,i}$, $i = 0, \ldots, n$ and λ is zero as follows

$$\partial L \Big/ \partial I_{b,i} = \partial J \Big/ \partial I_{b,i} - \lambda = 0 \tag{17a}$$

$$\partial L \Big/ \partial \lambda = \sum_{i=0}^{n} I_{D,i} - \sum_{i=0}^{n} I_{b,i} = 0 \tag{17b}$$

That is, in order to minimize the total power losses in the nano-grid, the necessary condition is to have the incremental loss rate, $\partial J / \partial I_{b,i}$ of all the batteries in the nano-grid the

same and equal to λ. From (17a), one can obtain λ_i for the *i*-th battery as follows

$$\lambda_i = 2\alpha_i I_{b,i} + \beta_i \tag{18}$$

Then by substituting (18) in (17b), $\lambda = \lambda_i$ is obtained as

$$\lambda = \left(\sum_{i=0}^{n} \frac{\beta_i}{2\alpha_i} + \sum_{i=0}^{n} I_{D,i}\right) \Big/ \sum_{i=0}^{n} \left(\frac{1}{2\alpha_i}\right) \tag{19}$$

The optimal charge and discharge current, $I^*_{b,i}$ and power, $P^*_{b,i}$ for the *i*-th battery can be obtained from (9b), (18) and (19) as

$$I^*_{b,i} = \left(\lambda - \beta_i\right)/2\alpha_i\,, \quad P^*_{b,i} = V_{dc,i} I^*_{b,i} \tag{20}$$

Lastly, taking the constraints given by (14c) into consideration, the optimal $P^*_{b,i}$ is modified as follows

$$P_{b,i} = \begin{cases} P^b_{max,i}\,, \text{ if } \quad V_{dc,i}\left(\lambda - \beta_i\right)/2\alpha_i > P^b_{max,i} \\ P^b_{min,i}\,, \text{ if } \quad V_{dc,i}\left(\lambda - \beta_i\right)/2\alpha_i < P^b_{min,i} \\ V_{dc,i}\left(\lambda - \beta_i\right)/2\alpha_i \quad \text{Otherwise.} \end{cases} \tag{21}$$

Consequently, $I^*_{b,i}$ which satisfies (14c) can be obtained from (21) as $I^*_{b,i} = P_{b,i}/V_{dc,i}$. However by including the battery constraints in (21), the equal incremental loss principle, $\lambda = \lambda_i$ required to minimize the total power losses may not work when one battery hits the limits given by (14c). The current balance constraint (14b) may also be unsatisfied when one battery hits its operation limits. To guarantee the optimality of the solution, λ is modified though the proposed FLIA:

$$\begin{cases} P^{(k+1)}_{b,i} & = V_{dc,i}\left(\lambda^{(k)} - \beta_i\right)/2\alpha_i \\ I^{(k+1)}_{b,i} & = P^{(k+1)}_{b,i}/V_{dc,i} \\ \Delta I^{(k+1)} & = \sum_{i=0}^{n}\left(I_{D,i} - I^{(k+1)}_{b,i}\right) \\ \lambda^{(k+1)} & = \lambda^{(k)} + e_\lambda \Delta I^{(k+1)} \\ v^{(k+1)}_{b,i} & = P^{(k+1)}_{b,i}/i_{b,i}\,, \quad \left(i_{b,i} = n_{b,i} I^{(k+1)}_{b,i}\right) \end{cases} \tag{22}$$

where k is the lambda iteration number, $\lambda^{(k)}$ is the approximated value of λ at iteration k and e_λ is a small positive number that defines the convergence speed of the FLIA.

From (22), if $\Delta I^{(k)} = 0$, it means that all batteries are 'active' i.e. operating without hitting their limits and the equal incremental loss principle applies. However, if $\Delta I^{(k)} \neq 0$, it means that certain 'inactive' batteries have hit their limits and their output power is either equal to zero or saturated at their absolute maximum values. To achieve $\Delta I^{(k)} = 0$ in this case, λ should be increased in the positive and negative direction respectively in order to compel the 'active' batteries to ramp up their charge/discharge rates more than the 'inactive' ones.

B. The Fast Voltage Iteration Algorithm

After $\mathbf{I_b}$ is obtained from the FLIA, distribution voltages $\mathbf{V_{dc}}$ can be obtained through the proposed FVIA:

$$\begin{cases} i_{dc,i} & = I_{D,i} - I_{b,i} \\ v^{(q+1)}_{bus} & = \left(\sum_{i=1}^{n} \frac{v^{(q)}_{dc,i}}{R_{dc,i}} - i_{dc,0}\right) \Big/ \sum_{i=1}^{n} \frac{1}{R_{dc,i}} \\ v^{(q+1)}_{dc,i} & = v^{(q+1)}_{bus} - i_{dc,i} R_{dc,i}\,, \quad i = 1, 2, \ldots, n \end{cases} \tag{23}$$

where q is the voltage iteration number and $v^{(q+1)}_{dc,i}$ is the updated approximation of the distribution voltage of household *i* with respect to the previous approximations of the distribution voltages, $v^{(q)}_{dc,j}$, $j = 0, 1, \ldots, n$ of other households *j*.

Taking the voltage limits (14d) into consideration, $v^{(q+1)}_{dc,i}$ obtained from (23) should satisfy the following voltage limits

$$v^{(q+1)}_{dc,i} = \begin{cases} v^{dc}_{max,i}\,, \text{ if } v^{(q+1)}_{bus} - i_{dc,i} R_{dc,i} > v^{dc}_{max,i} \\ v^{dc}_{min,i}\,, \text{ if } v^{(q+1)}_{bus} - i_{dc,i} R_{dc,i} < v^{dc}_{min,i} \\ v^{(q+1)}_{bus} - i_{dc,i} R_{dc,i} \text{ Otherwise.} \end{cases} \tag{24}$$

The FVIA given by (23) eliminates singularities that tend to be inherent in linear system of equations.

Due to voltage limits given by (24), its clear that 'new' distribution currents (25) obtained by voltage values at convergence of FVIA may be either equal (when voltage limits are not exceeded) or not equal (when voltage limits are exceeded) to distribution line currents calculated by (11).

$$i_{r,i} = \begin{cases} \left(v^{q\to\infty}_{bus} - v^{q\to\infty}_{dc,i}\right)/R_{dc,i}\,, \quad \text{if } \; i \neq 0 \\ -\sum_{i=1}^{n}\left(v^{q\to\infty}_{bus} - v^{q\to\infty}_{dc,i}\right)/R_{dc,i}\,, \quad \text{Otherwise.} \end{cases} \tag{25}$$

That is, $i_{r,i}$ given by (25) is equal to $i_{dc,i}$ given by (11) if and only if $v_{bus}, v_{dc,i}$ obtained from (23) are within voltage limits given by (24). Otherwise, $i_{r,i}$ is less than $i_{dc,i}$ and the excess current, $(I_{nr,i} = i_{dc,i} - i_{r,i})$ must be either discharged (if $i_{dc,i} > 0$) or charged (if $i_{dc,i} < 0$) by the *i*-th battery. However, in the case where battery limits given by (21) are reached, the excess, $i_{nr,i}$ denotes the proportion of $I_{D,i}$ that should be reduced through solar curtailment or load shedding.

Solar power generation is curtailed if $I_{D,i} < 0,\ i_{dc,i} < 0,\ P_{b,i} \geq P^b_{max,i}$ and $i_{nr,i} \neq 0$. Amount of power curtailed can be calculated as $P_{curtail} = i_{nr,i} v_{dc,i}$. Demand is load shed (reduced) if $I_{D,i} > 0, i_{dc,i} \geq 0, P_{b,i} \leq P^b_{min,i}$. Actual implementation of solar curtailment and load shedding is beyond scope of this paper.

C. Centralized Control Algorithm

The proposed algorithm which consists of the FLIA and FVIA can be implemented as given by Algorithm 1. Optimality proof of the FLIA is given in the Appendix. At every time step, data which include initial SoC, generation, demand and distribution line resistance is collected from all the households via communication links to a central location where the algorithm is computed. The distribution voltages are initialised to either values obtained at the previous time step or are set to the nominal distribution voltage values, $V_{dc,n}$. Using the initialised voltages, the FLIA is computed to obtain the optimal battery currents and power. With the optimal battery currents, the FVIA is evaluated to obtain new distribution voltages. The centralized control algorithm is terminated when the new distribution voltages are equal to the voltages obtained at the previous iteration. After convergence, excess demand/generation is either loadshed or curtailed respectively, and the battery SoCs are updated. The output of the algorithm are the final distribution voltages, which can be sent to the FPCs as control signals.

Algorithm 1 Centralized Control Algorithm

Collect data: $SoC_{o,i}$, $P_{pv,i}$, $P_{L,i}$ & $R_{dc,i}$ $\forall i = 0, 1, \ldots, n$
Initialize $V_{dc,i}^{(m)} = V_{dc,n}$ $i = 1, 2, \ldots, n$ and done1 = False
while not done1 **do**
  Evaluate (15a), (15b) & (15c) for $i = 0, 1, \ldots, n$
  Initialize $\lambda^{(k)}$ using (19), $e_\lambda \in (0, 1]$ and done2 = False
  Perform the FLIA algorithm:
  while not done2 **do**
    Evaluate the FLIA given by (22) and (21)
    if $|\lambda^{(k+1)} - \lambda^{(k)}| \leq 0.001$ **then**
      done2 = True
    else
      Update $\lambda^{(k)} \leftarrow \lambda^{(k+1)}$
      Update $e_\lambda \leftarrow 0.8e_\lambda$ (0.8 is a decay factor of e_λ)
      done2 = False
    end if
  end while
  Set $I_{b,i} \leftarrow I_{b,i}^{(k+1)}$ for $i = 0, 1, \ldots, n$
  Initialise, $v_{dc,i}^{(q)} = V_{dc,i}^{(m)}$, $v_{b,i}^{(q)} = v_{b,n}$ and done3 = False
  Perform the FVIA algorithm:
  while not done3 **do**
    Evaluate the FVIA given by (23) and (24)
    if $|v_{dc,i}^{(q+1)} - v_{dc,i}^{(q)}| \leq 0.001$ **then**
      done3 = True
    else
      Update $v_{dc,i}^{(q)} \leftarrow v_{dc,i}^{(q+1)}$
      done3 = False
    end if
  end while
  Set $V_{dc,i}^{(m+1)} \leftarrow v_{dc,i}^{(q+1)}$ for $i = 0, 1, \ldots, n$
  if $|V_{dc,i}^{(m+1)} - V_{dc,i}^{(m)}| \leq 0.001$ **then**
    done1 = True
  else
    Update $V_{dc,i}^{(m)} \leftarrow V_{dc,i}^{(m+1)}$
    done1 = False
  end if
end while
Calculate $i_{r,i}$ (25) and loadshed/curtail generation
Update battery SoC using (5)

V. Simulation Results

The performance of the proposed control algorithm was fully tested with a nano-grid which consists of four households ($n = 4$) and a hub as shown in Fig. 1. Battery and line parameters of the nano-grid are given in Table II. FPC simulation parameters are listed in [4]. The $v_{min,i}^{dc}$ and $v_{max,i}^{dc}$ were taken as 100 V and 120 V, $\forall i = 0, 1, \ldots, n$ respectively. $P_{c,i}^{+}$ and $P_{c,i}^{-}$ were taken as -120 W and 120 W, $\forall i = 0, 1, \ldots, n$ respectively. The $SoC_{min,i}$ and $SoC_{max,i}$ were 20% and 95%, $\forall, i = 0, 1, \ldots, n$ respectively. The batteries in the households and hub were assumed to have equal initial SoC of 50%. A 2×250 W, 24 V solar panel [29] was used at H0. Two case studies were investigated in order to verify the performance of the proposed algorithm. In the first case study, constant values of power generation and load demand were used. The objective of this case study was to investigate the convergence of the FLIA and FVIA. In the second case study, time-varying values of household/hub power generation and load demand were used. The objective of this study was to verify the effectiveness of the proposed algorithm for: 1) facilitating power exchange between the households and hub while strictly satisfying the operational constraints and 2) minimising the total energy losses of the nano-grid.

TABLE II
Battery and Line Parameters.

	H0	H1	H2	H3	H4
$C_{b,i}$ (kWh)	0.96	1.32	0.66	1.80	0.80
$R_{dc,i}$ (Ω)	0.0	3.0	2.0	1.5	3.0
$V_{dc,n}$ (V)	110	110	110	110	110
$V_{n,i}^{b}$ (V)	12	12	12	12	12

A. CASE STUDY 1: With Constant Demand and Solar Power

In this case study, values of power generation and load demand were taken as constants, thus representing a specific operating point of the solar nano-grid. For the purpose of this case study, constant power generation (at H0) was equal to 500 W and the constant load demand values at H0, H1, H2, H3 and H4 were set to be 100 W, 50 W, 80 W, 80 W and 80 W respectively. Distribution voltages were considered to have nominal values (see Table II). Other calculated parameters are summarised in Table III. In the next subsections, convergence analysis of the FLIA and FVIA is presented.

TABLE III
Additional simulation parameters for case study 1.

	H0	H1	H2	H3	H4
$I_{D,i}$ (A)	-3.64	0.45	0.73	0.73	0.73
α	0.52	3.38	2.76	1.78	3.28
β	0	-2.73	-2.91	-2.18	-4.36
r_b (mΩ)	6.2	4.5	9.0	3.3	3.3

Convergence of the Fast Lambda Iteration Algorithm

Fig. 6 showed that convergence of the FLIA was achieved within six iterations. At convergence, the total mismatch current in the nano-grid was zero. This showed that the proposed FLIA converges and achieves the current balance in the nano-grid. The value of λ at convergence was equal to -2.77 W/A. The optimal battery charge and discharge currents corresponding to $\lambda = -2.77$ W/A were -1.091 A, -0.007 A, 0.024 A, -0.168 and 0.242 A for H0, H1, H2, H3 and H4 respectively.

Convergence of the Fast Voltage Iteration Algorithm

The distribution line currents for H0, H1, H2, H3 and H4 corresponding to the optimal battery charge and discharge currents obtained from the FLIA in the previous subsection were obtained from (11) as -2.545 A, 0.462 A, 0.703 A, 0.895 A and 0.485 A respectively. These values were then used to determine the convergence of the FVIA as shown in Fig. 6b. Fig. 6b showed that FVIA converges after one iteration. This was always the case provided that the distribution line currents were balanced.

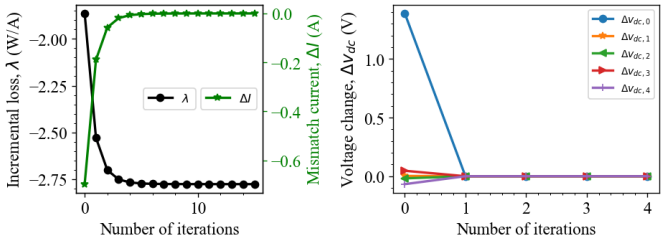

(a) (b)

Fig. 6. Convergence speed of (a) FLIA and (b) FVIA.

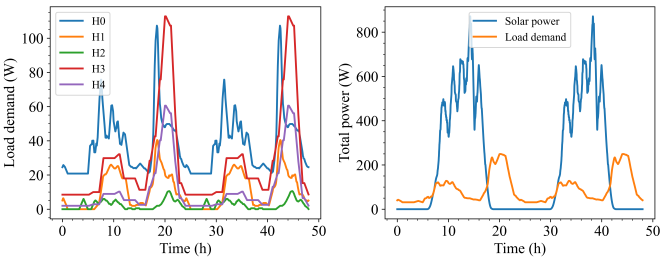

(a) (b)

Fig. 7. 48 h (a) household load demand profiles and (b) total solar power generation and total load demand.

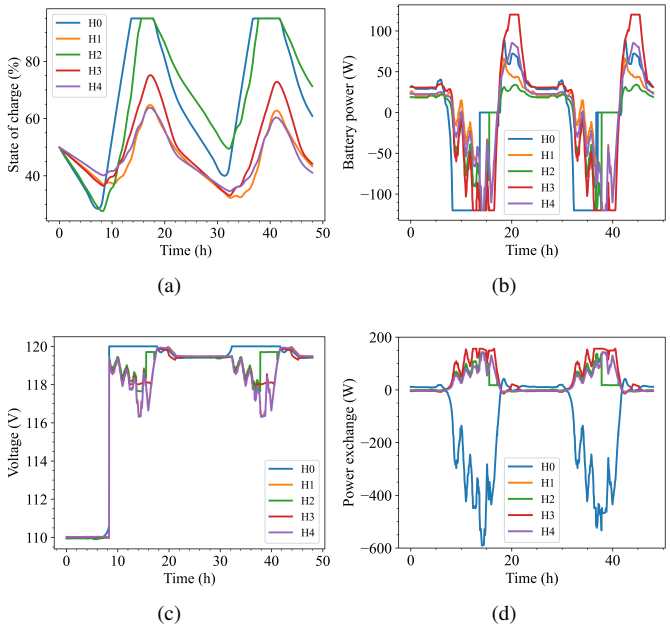

(a) (b) (c) (d)

Fig. 8. Power management performance of the proposed centralized control algorithm with solar panels at the hub only: (a) battery SoC, (b) battery charge and discharge power, (c) distribution voltages and (d) power exchange.

B. CASE STUDY 2: With Varying Demand and Solar Power

In this case study, the performance of the proposed centralized control algorithm (see, Algorithm 1) for time varying load demand and solar panel output power is presented. The performance of the proposed algorithm was evaluated for two case studies, A-and B with different locations of solar panels. In case study A, only the hub had solar panels and in case study B, both the hub and H4 had solar panels. It should be noted that H4 was chosen for simulation purposes only and any other household could have been chosen to serve the same purpose without affecting the analysis of the results.

CASE STUDY A: Solar Panels at the Hub Only

The considered load demand profiles [30] for the households and hub are shown in Fig. 7a. The total load demand and solar power generation profiles are shown in Fig. 7b. The simulation results are shown in Fig. 8. Fig. 8a and Fig. 8b showed that the proposed algorithm can coordinate the charge and discharge operation of the batteries while keeping the battery output power within ± 120 W and the battery SoC between 20% and 95%. The battery at H0 charged faster than other batteries for most periods because it was situated near the solar panels. This was followed by the battery at H2 owing to its relative small capacity. With reference to Fig. 7b, it can be observed in Fig. 8b that the nano-grid batteries charged the excess and deficit solar power generation to meet the total load demand. Fig. 8c and Fig. 8d showed that the proposed algorithm effectively facilitated the power exchange between the households while keeping the voltages within their limits.

CASE STUDY B: Solar Panels at Both the Hub and Household

The purpose of this case study was to evaluate the performance of the proposed algorithm in a case where a household in the nano-grid also had solar panels. Here, H4 was considered to have solar panels with capacity equal to those at H0. The simulation results in Fig. 9 showed that the proposed algorithm also works in a case where households have solar panels installed.

As expected, Fig. 9 showed that by installing solar panels at the households in addition to the hub increases the amount of power stored in the batteries. This is shown by battery SoCs in Fig. 9a, where they reached maximum values.

However, installing solar panels at the households (thus increasing the solar power generation in the nano-grid) was observed to increase both battery and distribution line losses as shown in Table IV. This is because of the increased amount of power stored in the batteries and additional power exchange from H4 between the households as shown by comparing Fig. 9d to Fig. 8d. In other words, the nano-grid power loss problem is largely driven by solar power generation. The higher the solar power generation, the higher the nano-grid power losses.

TABLE IV
COMPARISON OF NANO-GRID ENERGY LOSS RESULTS.

	Solar at H0	Solar at H0 & H4
Battery loss (Wh)	22.74	28.73
Distribution loss (Wh)	99.02	147.77
FPC loss (Wh)	4426.44	4426.44
Total energy loss (Wh)	**4548.24**	**4602.94**

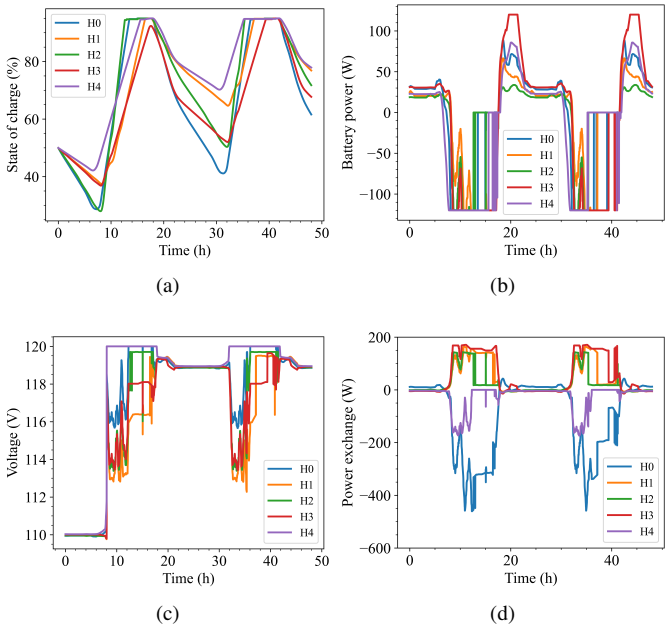

Fig. 9. Power management performance of the proposed centralized control algorithm with solar panels at both the hub and H4: (a) battery SoC, (b) battery charge and discharge power, (c) distribution voltages and (d) power exchange.

C. Power Loss Comparison Between the Proposed Algorithm and Existing Method

To validate the performance of the proposed algorithm, the nano-grid energy loss results obtained for case study A in the previous subsection were compared to those obtained through an existing method given in [8]. The existing approach involves formulating the power loss optimization problem of the nano-grid through linearisation of power flow equations and then solving the problem using a software package. Table V compares the total energy loss of the nano-grid obtained through the proposed algorithm and the existing approach. As shown in Table V, the proposed algorithm had improved

TABLE V
COMPARISON OF NANO-GRID ENERGY LOSS RESULTS BETWEEN EXISTING AND THE PROPOSED APPROACH.

	Existing Method	Proposed Algorithm
Battery loss (Wh)	32.44	22.74
Distribution loss (Wh)	123.75	99.02
FPC loss (Wh)	4426.44	4426.44
Total energy loss (Wh)	**4582.63**	**4548.24**
Total execution time (s)	86.49	69.21

energy loss results and execution time compared to the existing approach. It is further noted from Table V that FPC losses account for the majority of the energy losses in the nano-grid, followed by distribution line losses and then the battery losses. Similar observation can be made in Table IV as well. This shows that neglecting the FPC loss can significantly affect the nano-grid operation. The FPC losses are the same for both methods because same load profiles were used and that the FPC loss is a function of load power as given in Section II-E.

Apart from being fast and accurate, the main advantage of the proposed approach compared to the existing method and other methods like heuristics methods [23] is that it lays a mathematical foundation on which advanced distributed control algorithms can be developed. In Part II of this paper, a distributed control algorithm is proposed which utilises the mathematical equations and insights developed in this paper. Moreover, the centralized algorithm proposed in this paper is more suited for small nano-grids in rural areas where privacy of households and computational burden of the centralized controller are not a concern. To take these concerns into account especially for large-scale nano-grids, a distributed control algorithm is proposed in Part II.

VI. CONCLUSION

A novel centralized control algorithm is developed in this paper to minimize power losses of a multi-port converter-enabled solar DC nano-grid that is designed for energy access. The algorithm is developed by first formulating the power loss problem as a two-stage convex optimization problem. The first stage is the OBDP for determining the optimal battery charge and discharge currents that minimize the nano-grid power losses. The second stage is the OCFP for determining the optimal distribution voltages that correspond to the battery charge and discharge currents from the OBDP. Then, two iterative algorithms, the FLIA and FVIA which together form the proposed centralized control algorithm are developed to solve the OBDP and OCFP respectively. Simulation results verify the effectiveness of the proposed algorithm for minimising the nano-grid power losses while satisfying operational constraints such as the battery SoC limits. FPC losses were found to be more than 20 times higher than the distribution line losses and more than 100 times higher than the battery losses. This suggests that converter losses are the majority in multi-port converter-enabled solar DC nano-grids. Furthermore, the nano-grid power loss problem was also found to be largely driven by solar power generation. The higher the generation, the higher the power losses. In part II of this paper, a distributed control algorithm will be proposed to address the privacy concerns of the proposed algorithm.

APPENDIX A
OPTIMALITY PROOF OF FLIA

The FLIA (22) iteratively solves the optimization problem stated by (14). Considering inequality constraints given by (14c), this problem can be converted to an unconstrained problem using the Lagrangian operator L as

$$L\left(I_{b,i},\lambda,\mu_i,\sigma_i\right)=J+\lambda\left(\sum_{i=0}^{n}I_{D,i}-\sum_{i=0}^{n}I_{b,i}\right)+\sum_{i=0}^{n}\mu_i\left(-I_{b,i}V_{dc,i}+P^b_{min,i}\right)+\sum_{i=0}^{n}\sigma_i\left(I_{b,i}V_{dc,i}-P^b_{max,i}\right) \tag{26}$$

In this appendix, we show that the convergence value of the FLIA (22) is optimal. Since (14) is convex, Karush-Kuhn-Tucker (KKT) optimality conditions are necessary and

sufficient conditions for optimality [28]. Thus, it suffices to show that the convergence value of the FLIA satisfies KKT conditions, which are:

$$\frac{\partial L}{\partial I_{b,i}}\Big|_{\substack{I^*_{b,i},\lambda^*,\\ \mu^*_i,\sigma^*_i}} = \frac{\partial J}{\partial I_{b,i}} - \lambda^* - V_{dc,i}\left(\mu^*_i - \sigma^*_i\right) = 0 \tag{27a}$$

$$\frac{\partial L}{\partial \lambda}\Big|_{\substack{I^*_{b,i},\lambda^*,\\ \mu^*_i,\sigma^*_i}} = \sum_{i=0}^{n} I_{D,i} - \sum_{i=0}^{n} I^*_{b,i} = 0 \tag{27b}$$

$$\frac{\partial L}{\partial \mu_i}\Big|_{\substack{I^*_{b,i},\lambda^*,\\ \mu^*_i,\sigma^*_i}} = -I^*_{b,i}V_{dc,i} + P^b_{min,i} = 0 \tag{27c}$$

$$\frac{\partial L}{\partial \sigma_i}\Big|_{\substack{I^*_{b,i},\lambda^*,\\ \mu^*_i,\sigma^*_i}} = I^*_{b,i}V_{dc,i} - P^b_{max,i} = 0 \tag{27d}$$

Convergence of the FLIA (22) depends on ΔI^k and the convergence factor e_λ as discussed in the last paragraph of Section IV-A. So long as $\Delta I^k \to 0$ as $k \to \infty$, $\lambda^{(k+1)} = \lambda^{(k)} = \lambda^*$ and the FLIA converges. Convergence of (22) can also be achieved by making $e_\lambda = (0, 1]$ to slowly decay towards zero at a constant rate as $k \to \infty$. The final value of $\lambda = \lambda^*$ however, depends on the amount of current and power each battery charges or discharges.

To prove optimality when $\lambda = \lambda^*$, satisfaction of the KKT conditions in (27) suffices. Clearly, $P^b_{max,i} \neq P^b_{min,i}$ and $(I_{b,i}V_{dc,i})$ cannot equal both $P^b_{max,i}$ and $P^b_{min,i}$, and equations (27c) and (27d) cannot both be satisfied. In this case we proceed by selecting a subset of the constraints, and evaluating the resulting solutions as follows:

- **Constraint 1:** $P^b_{min,i} < \left(I^*_{b,i}V_{dc,i}\right) < P^b_{max,i}$
  In this case, setting $\mu_i = \sigma_i = 0$ (i.e. ignoring the inequality constraints of equation (14)) satisfies the KKT conditions given in (27a), (27c) and (27d). Here, optimal λ^* and $I^*_{b,i}$ are evaluated as given by (19) and (20) respectively.
- **Constraint 2:** $P^b_{min,i} > \left(I^*_{b,i}V_{dc,i}\right)$
  This is a case where battery's minimum power constraint is exceeded and to protect the battery and converter from damage, $\left(I^*_{b,i}V_{dc,i}\right)$ is taken as $\left(I^*_{b,i}V_{dc,i}\right) = P^b_{min,i}$. Setting $\sigma_i = 0$, μ_i can be obtained from (14a) & (27a) as
  $$\mu_i = \frac{1}{V_{dc,i}}\left(2\alpha_i\frac{P^b_{min,i}}{V_{dc,i}} + \beta_i - \lambda^*\right) > 0 \tag{28}$$
  which satisfies the KKT conditions in (27a), (27c) and (27d).
- **Constraint 3:** $P^b_{max,i} < \left(I^*_{b,i}V_{dc,i}\right)$
  In this case, battery's maximum power limit is exceeded and to protect the battery and converter from damage, $\left(I^*_{b,i}V_{dc,i}\right)$ is taken as $\left(I^*_{b,i}V_{dc,i}\right) = P^b_{max,i}$. By taking $\mu_i = 0$, σ_i which satisfies the KKT conditions in (27a), (27c) and (27d) can be obtained from (14a) & (27a) as
  $$\sigma_i = \frac{1}{V_{dc,i}}\left(\lambda^* - 2\alpha_i\frac{P^b_{max,i}}{V_{dc,i}} + \beta_i\right) > 0 \tag{29}$$

Thus, for any convergence value of FLIA i.e. $\lambda = \lambda^*$, there exists a set of μ_i and σ_i, $\forall i = 0, 1 \ldots, n$ which satisfies the KKT conditions. Since the problem formulation given by (14) is convex with affine constraints, its solution is therefore a global optimal [28].

It should be noted that (27b) is satisfied even for **Constraints** 2 and 3 provided that not every battery in the nano-grid operates at maximum values as explained in Section IV-A. Otherwise (27b) is not satisfied and excess solar generation and demand should be curtailed and load-shed respectively.

Appendix B
Convergence Analysis of FVIA

The convergence analysis and initialization of the FVIA can be analysed by rewriting (23) in a matrix form as follows

$$\mathbf{V_{dc}}^{(q+1)} = \mathbf{W}\mathbf{V_{dc}}^{(q)} + \mathbf{c} \tag{30}$$

where $\mathbf{V_{dc}}^{(q)} = \left[v^{(q)}_{dc,i}, \ldots, v^{(q)}_{dc,n}\right]^T$, $\mathbf{W} = (w_{ij})_{n\times n}$, and

$$\mathbf{c} = -\left[\frac{i_{dc,0}}{\sum_{i=1}^{n} R_{dc,i}} + R_{dc,1}i_{dc,1}, \ldots, \frac{i_{dc,0}}{\sum_{i=1}^{n} R_{dc,i}} + R_{dc,n}i_{dc,n}\right]^T \tag{31}$$

The matrix $\mathbf{W}$ has the following characteristics:

- $w_{ij} = \frac{1}{R_{dc,j}}\sum_{i=1}^{n} R_{dc,i} > 0$, $\forall i, j = 1, 2, \ldots, n$,
- $\sum_{j=1}^{n} w_{ij} = 1$, $\forall i = 1, 2, \ldots, n$,
- $\mu_1 = 1$ is a simple eigenvalue of $\mathbf{W}$ and all other eigenvalues; $\mu_2, \ldots, \mu_n$ are zero,
- $\mathbf{1} = [1, \ldots, 1]^T$ is a right eigenvector of $\mathbf{W}$ associated with $\mu_1 = 1$, i.e. $\mathbf{W1} = \mathbf{1}$,
- $\pi_\mathbf{w} = [w_{i1}, w_{i2}, \ldots, w_{in}]$, $i = 1, 2, \ldots, n$ is a left eigenvector of $\mathbf{W}$ associated with $\mu_1 = 1$, i.e. $\pi_\mathbf{w}\mathbf{W} = \pi_\mathbf{w}$.

The above characteristics verify that $\mathbf{W}$ is a row stochastic matrix and according to Perron-Frobenius theorem [31], the convergence of $\mathbf{W}$ and the convergence of the FVIA algorithm thereof exists.

Pre-multiplying (30) by $\pi_\mathbf{w}$, the following expression can be obtained

$$\pi_\mathbf{w}\mathbf{V_{dc}}^{(q+1)} = \pi_\mathbf{w}\mathbf{W}\mathbf{V_{dc}}^{(q)} + \pi_\mathbf{w}\mathbf{c} \tag{32}$$

Noticing that $\pi_\mathbf{w}\mathbf{W} = \pi_\mathbf{w}$ and that $\pi_\mathbf{w}\mathbf{c} = -\left(\sum_{i=0}^{n} i_{dc,i}\right)/\sum_{i=1}^{n}\frac{1}{R_{dc,i}}$, the expression given by (32) can be further simplified as follows

$$\pi_\mathbf{w}\left[\mathbf{V_{dc}}^{(q+1)} - \mathbf{V_{dc}}^{(q)}\right] = -\frac{\sum_{i=0}^{n} i_{dc,i}}{\sum_{i=1}^{n}\frac{1}{R_{dc,i}}} \tag{33}$$

or, equivalently

$$\sum_{i=1}^{n} v^{(q+1)}_{dc,i} - \sum_{i=1}^{n} v^{(q)}_{dc,i} = -R_{dc,i}\sum_{i=0}^{n} i_{dc,i} \tag{34}$$

As $\sum_{i=0}^{n} i_{dc,i} = 0$ after convergence of the FLIA, taking limits on both sides of (34) as $q \to \infty$ yields the following expression

$$\lim_{q\to\infty}\sum_{i=0}^{n} v^{(q+1)}_{dc,i} = \lim_{q\to\infty}\sum_{i=0}^{n} v^{(q)}_{dc,i} \tag{35}$$

That is, as $q \to \infty$, the difference between $v_{dc,i}^{(q+1)}$ and $v_{dc,i}^{(q)}$ is approximately equal to zero and the FVIA converges for any choice of initial values, $\mathbf{V_{dc}}^{(0)} = \left[v_{dc,1}^{(0)}, \ldots, v_{dc,n}^{(0)}\right]^T$.

APPENDIX C
OPTIMALITY PROOF OF THE CENTRALIZED CONTROL ALGORITHM

We analyse the existence of a fixed point to prove the optimality of the proposed centralized control algorithm. As (14a) is a strictly convex function of $\mathbf{I_b}$, the optimal value of $\mathbf{I_b}$ is a one-to-one correspondence to the distribution voltage $\mathbf{V_{dc}}$ calculated through the FVIA (23). That is, $\mathbf{I_b}$ is a function of $\mathbf{V_{dc}}$: $\mathbf{I_b} = F(\mathbf{V_{dc}})$. Further, according to (23), the relationship between $\mathbf{I_b}$ and $\mathbf{V_{dc}}$ can be expressed as $\mathbf{V_{dc}} = G(\mathbf{I_b})$. Thus, the whole centralized control algorithm can be described as $\mathbf{V_{dc}} = G(F(\mathbf{V_{dc}})) = H(\mathbf{V_{dc}})$. As F and G are compact and continuous functions, H is also a compact and continuous function.

Theorem (Brouwer Fixed-Point Theorem): Let X be bounded, closed and a non-empty compact convex set in R^N and f be a compact and continuous function mapping X into itself, i.e. $f : X \to X$. Then f has a fixed point X^* [32].

As $\mathbf{V_{dc}} \in D$ where $D = \left[v_{min,i}^{dc}, v_{max,i}^{dc}\right]$ and $H : D \to D$, according to the **Theorem** there exists a fixed point in D for $H(\mathbf{V_{dc}})$. Thus, if the algorithm converges to a fixed point after a finite number of iterations, the distribution voltage $\mathbf{V_{dc}}$ converges and the obtained solution is optimal. Otherwise, it is divergent, the optimization problem is unsolvable and the households still can satisfy their energy demands using the on-site batteries.

REFERENCES

[1] F. F. Nerini, O. Broad, D. Mentis, M. Welsch, M. Bazilian, and M. Howells, "A cost comparison of technology approaches for improving access to electricity services," *Energy*, vol. 95, pp. 255–265, 2016.

[2] H. Kirchhoff and K. Strunz, "Key drivers for successful development of peer-to-peer microgrids for swarm electrification," *Applied Energy*, vol. 244, pp. 46–62, 2019.

[3] N. Narayan, A. Chamseddine, V. Vega-Garita, Z. Qin, J. Popovic-Gerber, P. Bauer, and M. Zeman, "Exploring the boundaries of solar home systems (shs) for off-grid electrification: Optimal shs sizing for the multi-tier framework for household electricity access," *Applied energy*, vol. 240, pp. 907–917, 2019.

[4] C. Samende, N. Mugwisi, D. J. Rogers, E. Chatzinikolaou, F. Gao, and M. McCulloch, "Power loss analysis of a multiport dc–dc converter for dc grid applications," in *IECON 2018-44th Annual Conference of the IEEE Industrial Electronics Society*, pp. 1412–1417, IEEE, 2018.

[5] H. Tao, A. Kotsopoulos, J. L. Duarte, and M. A. M. Hendrix, "Family of multiport bidirectional dc-dc converters," *IEE Proceedings - Electric Power Applications*, vol. 153, no. 3, pp. 451–458, 2006.

[6] N. Narayan, A. Chamseddine, V. Vega-Garita, Z. Qin, J. Popovic-Gerber, P. Bauer, and M. Zeman, "Quantifying the benefits of a solar home system-based dc microgrid for rural electrification," *Energies*, vol. 12, no. 5, p. 938, 2019.

[7] M. Nasir, H. A. Khan, A. Hussain, L. Mateen, and N. A. Zaffar, "Solar pv-based scalable dc microgrid for rural electrification in developing regions," *IEEE Transactions on sustainable energy*, vol. 9, no. 1, pp. 390–399, 2017.

[8] T. Morstyn, B. Hredzak, R. P. Aguilera, and V. G. Agelidis, "Model predictive control for distributed microgrid battery energy storage systems," *IEEE Transactions on Control Systems Technology*, vol. 26, no. 3, pp. 1107–1114, 2017.

[9] International Energy Agency, "Energy efficiency 2019, IEA, paris," 2019.

[10] Y. Saito, M. Shikano, and H. Kobayashi, "Heat generation behavior during charging and discharging of lithium-ion batteries after long-time storage," *Journal of Power Sources*, vol. 244, pp. 294–299, 2013.

[11] L. Gan and S. H. Low, "Optimal power flow in direct current networks," *IEEE Transactions on Power Systems*, vol. 29, no. 6, pp. 2892–2904, 2014.

[12] K. Unger, "Organically grown microgrids: The development and simulation of a solar home system-based microgrid," Master's thesis, University of Waterloo, 2012.

[13] P. Hollberg, "Swarm grids-innovation in rural electrification," Master's thesis, 2015.

[14] L. Strenge, "Modeling and simulation of a droop controlled swarm type low voltage dc microgrid in a dae framework," Master's thesis, 2015.

[15] S. Groh, D. Philipp, B. E. Lasch, and H. Kirchhoff, "Swarm electrification: Investigating a paradigm shift through the building of microgrids bottom-up," in *Decentralized Solutions for Developing Economies*, pp. 3–22, Springer, 2015.

[16] A. Magnasco, H. Kirchhoff, S. Chowdhury, and S. Groh, "Data services for real time optimization of dc nanogrids with organic growth," *Energy Procedia*, vol. 103, pp. 369–374, 2016.

[17] M. Nasir, S. Iqbal, and H. A. Khan, "Optimal planning and design of low-voltage low-power solar dc microgrids," *IEEE Transactions on Power Systems*, vol. 33, no. 3, pp. 2919–2928, 2017.

[18] C. Samende, S. M. Bhagavathy, F. Gao, and M. McCulloch, "Decentralized voltage control for efficient power exchange in interconnected dc clusters," *IEEE Transactions on Sustainable Energy*, pp. 1–13, 2020.

[19] T. Dragičević, X. Lu, J. C. Vasquez, and J. M. Guerrero, "Dc microgridspart ii: A review of power architectures, applications, and standardization issues," *IEEE transactions on power electronics*, vol. 31, no. 5, pp. 3528–3549, 2015.

[20] M. Aragüés-Peñalba, A. Egea-Àlvarez, O. Gomis-Bellmunt, and A. Sumper, "Optimum voltage control for loss minimization in hvdc multi-terminal transmission systems for large offshore wind farms," *Electric power systems research*, vol. 89, pp. 54–63, 2012.

[21] C. Ahn and H. Peng, "Decentralized voltage control to minimize distribution power loss of microgrids," *IEEE Transactions on Smart Grid*, vol. 4, no. 3, pp. 1297–1304, 2013.

[22] W. Saad, Z. Han, and H. V. Poor, "Coalitional game theory for cooperative micro-grid distribution networks," in *2011 IEEE international conference on communications workshops (ICC)*, pp. 1–5, IEEE, 2011.

[23] J.-H. Teng, S.-W. Luan, D.-J. Lee, and Y.-Q. Huang, "Optimal charging/discharging scheduling of battery storage systems for distribution systems interconnected with sizeable pv generation systems," *IEEE Transactions on Power Systems*, vol. 28, no. 2, pp. 1425–1433, 2012.

[24] L. Cristaldi, M. Faifer, M. Rossi, and S. Toscani, "An improved model-based maximum power point tracker for photovoltaic panels," *IEEE Transactions on Instrumentation and Measurement*, vol. 63, no. 1, pp. 63–71, 2013.

[25] C. Cresswell, *Steady state load models for power system analysis*. PhD thesis, University of Edinburgh, 2009.

[26] T. Kim and W. Qiao, "A hybrid battery model capable of capturing dynamic circuit characteristics and nonlinear capacity effects," *IEEE Transactions on Energy Conversion*, vol. 26, no. 4, pp. 1172–1180, 2011.

[27] S. Diamond and S. Boyd, "Cvxpy: A python-embedded modeling language for convex optimization," *The Journal of Machine Learning Research*, vol. 17, no. 1, pp. 2909–2913, 2016.

[28] S. Boyd, S. P. Boyd, and L. Vandenberghe, *Convex optimization*. Cambridge university press, 2004.

[29] Suntech, "250 w monocrystalline solar module," 2012.

[30] N. Nishant, "Electrical power consumption load profiles for households with dc appliances related to multi-tier framework for household electricity access," 2018.

[31] H. Perfect and L. Mirsky, "Spectral properties of doubly-stochastic matrices," *Monatshefte für Mathematik*, vol. 69, no. 1, pp. 35–57, 1965.

[32] S. Park, "Ninety years of the brouwer fixed point theorem," *Vietnam J. Math*, vol. 27, no. 3, pp. 187–222, 1999.